Available online at www.sciencedirect.com
ScienceDirect
Journal of the European Ceramic Society 32 (2012) 277–282
www.elsevier.com/locate/jeurceramsoc

Copper based hydrophobic ceramic nanocoating

J.J. Reinosa [a,*], J.J. Romero [a], P. Jaquotot [b], M.A. Bengochea [c], J.F. Fernández [a]

[a] *Electroceramic Department, Instituto de Ceramica y Vidrio, CSIC, Madrid 28049, Spain*
[b] *Kerafrit S.A., 12520 Nules, Castellón, Spain*
[c] *Grupo Keraben S.A., 12520 Nules, Castellón, Spain*

Received 25 February 2011; received in revised form 1 August 2011; accepted 7 August 2011
Available online 7 September 2011

Abstract

A mechanism for the development of nanocoatings for the tiles industry by using copper nanoparticles has been proposed. A standard processing procedure in which ceramics were fast-firing at 1200 °C in air atmosphere simulating an industrial process was followed. The ceramic nanocoating was multifunctional having shine metallic aspect and hydrophobic characteristics. The surface crystallizations were studied by X-ray diffraction and corresponded to copper oxide nanocrystals. The hydrophobic response was based in the nanoroughness of the surface and correlated with the Cu^{+}/Cu^{2+} ratio as determined by XANES. The cellular nano microstructure look biomimetic with the one of hydrophobic leafs. The development of the cellular nano microstructure was based on the Rayleigh–Bernard cells of a saturated glass during cooling in which thermal convection currents allow the crystallization of nanoparticles at the surface of the glass.

Keywords: B. Microstructure-final; E. Functional applications; Nanostructure-final; Hydrophobicity; Glaze

1. Introduction

Since IX century A.D., glazes with bright metallic shine have been characterized by a high decorative value. Ceramic luster is a reduced-pigmented glaze[1] showing a golden or coppery metallic shine that exhibits purple and blue iridescence.[2,3] Luster is defined[4] as a nanosized metal–glass composite made of copper and/or silver nanoparticles embedded in a glassy matrix. One peculiar optical property of this kind of coating is its capability of reflecting light like a continuous metal surface.[5] Luster is produced following a well known process consisting of the application of copper and silver based paint to an already glazed ceramic substrate, and a further low temperature firing 600 °C.[1] The firing process takes place under a reducing atmosphere, during which silver and copper ions are incorporated into the glaze via an ionic exchange mechanism.[6] The result is a thin coating of copper and/or silver metallic nanoparticles.

Recently, multifunctional hydrophobic surfaces have been widely demanded for potential applications in interdisciplinary technological fields, including microelectronics, biosensors, smart structural coating materials and microfluidics.[7]

Hydrophobic and super-hydrophobic surfaces have attracted significant attention during the last few years due to their intriguing properties and their important industrial applications.[8] In this field many researchers are inspired by the so-called "Lotus effect" and attempt to mimic the structural design of natural super-hydrophobic leaves.[9] It is described that the combination of nano and microstructures at the surface of the petals and leaves of the Lotus Flower plant generates the phenomenon of super-hydrophobicity, which helps to clean the leaves surface from dust and contaminants.[10]

In this study we describe the mechanism of formation of a multifunctional ceramic coating for ceramic tiles[11] following a standard method used by the ceramic industry that consists on one single sintering step in air atmosphere at high temperature (1200 °C). This process, based on copper addition to the glaze, is a challenge for the technological advance of the tile sector.

The use of Cu metallic particles in the glaze processing is not feasible because of their high density and flocculation in slip that resulted in non homogeneous materials. Cu metal-

* Corresponding author at: Electroceramic Department, Instituto de Ceramica y Vidrio, CSIC, Madrid, 28049 Spain. Tel.: +34 91 735 58 40; fax: +34 91 735 58 43.
E-mail address: jjreinosa@icv.csic.es (J.J. Reinosa).

0955-2219/$ – see front matter © 2011 Elsevier Ltd. All rights reserved.
doi:10.1016/j.jeurceramsoc.2011.08.013

lic nanoparticles could minimize this problem but in practice the high agglomeration state of nanoparticles impede their use. To avoid such a problem, sepiolite nanofiber clay was used to support the Cu metallic nanoparticles.[12]

2. Experimental procedure

Homogeneous glaze suspensions of commercial frit, Kaolin and metallic copper in water were performed. The solid content was 40 wt.% of the total mass and the relative proportions of the main components of the glazes were, in weight %: 93 frit/7 kaolin. The frit corresponds to an industrial standard used for stoneware ceramic tiles supplied by Kerafrit S.A. Metallic copper nanoparticles were supported in sepiolite nanofibers supplied by TOLSA. The methodology to attach the metallic nanoparticles to sepiolite was previously described.[13] The metallic copper was added to the prepared glaze on proportions corresponding to 5, 10, 15, 20 and 25 wt.% of the total mass of the glaze. These compositions will be named hereafter S5, S10, S15, S20 and S25, respectively.

The glaze suspension was homogenized by ball milling in porcelain jars with sodium trypolyphosphate as deflocculant and carboximethyl cellulose to improve the adhesive behavior of the glaze to green stoneware substrate. After milling operations, prepared glaze suspensions were sieved through a 63 μm sieve. After that, the suspension was sprayed on the surface of a green stoneware tile producing layer of about 150 μm. The tiles with the glaze layer were dried at 90 °C and fast-fired in a conventional industrial furnace (Pirometrol) in a 55 min thermal cycle, the soaking temperature being 1200 °C for 5 min in air atmosphere. This sintering cycle corresponds to a standard industrial fast-firing process of stoneware tiles.

The ceramic glaze surfaces were characterized by a DTA/TG analysis in air at a heating rate of 10 °C/min. The crystalline phases were studied by X-ray diffraction analysis which was performed with a graphite monochromatic CuKα radiation and a Ni filter, operating at 50 kV, 30 mA and a step-scan of 0.02°, using a Siemens D500 Diffractometer in grazing angle. The surface was observed using a polarized light optical microscope, Zeiss Axiophot, equipped with a Zeiss Axiocam MRC5. The microstructure was studied by a Field Emission Scanning Electron Microscope FE-SEM, Hitachi S-4700, with a resolution of 1.5 nm at 20 kV. The nanostructure was studied by transmission electronic microscope (TEM) with a Hitachi H-7100 microscope, and the water contact angle was measured with the drop shape analysis system Easy Drop Standard from Krüss. X-ray absorption spectroscopy was performed for the Cu K-edge (8979 eV) on the Spanish beamline SPLINE of the European sincrotron radiation facility (ESRF).

3. Results and discussion

To obtain the metallic effect, glazes with different concentrations of sepiolite-suported metallic copper nanoparticles were used. Layers of about 150 μm were applied over green stoneware tiles. After firing, yellowish and greenish glazes were obtained for compositions S5 and S10, respectively. It was reported that

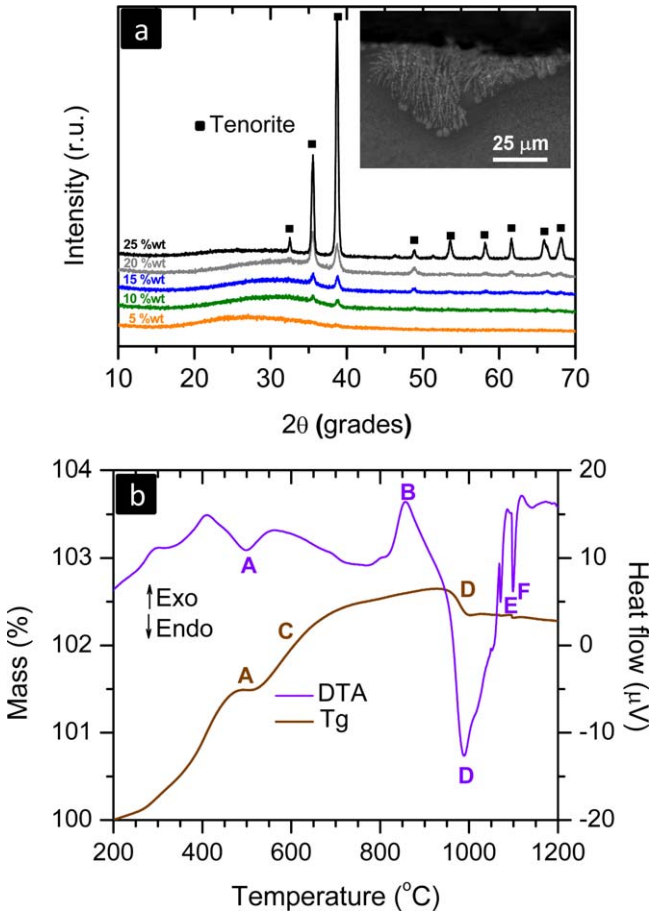

Fig. 1. (a) XRD of the glazes surface; CuO as Tenorite is the unique crystalline phase found in the samples. In the inset an optical micrograph shows the crystallization of Tenorite near the surface of the sample S25. (b) DTA/TG of the glaze powder S15. TG line shows the evolution of the copper (a gradual oxidation and its reduction) during the thermal treatment.

these colors in glassy phases are due to the presence of Cu^{2+} acting as a network modifier.[14] The observed green color is related to a cupric absorption band located near 780 nm ascribed to the $^2Eg \rightarrow {}^2Tg$ transition of Cu^{2+} ions coordinated octahedrally with the oxygen ions.[15,16] It is also described that the octahedrons are tetragonally distorted due to Jahn–Teller effect.[17]

Bright metallic effect is observed for S15 whereas S20 and S25 show matt metallic effects corresponding with rough surfaces. The roughness was attributed to the segregation of copper from the glassy matrix because of its saturation. In fact, X-ray diffraction determined a gradual increase of crystalline CuO as Tenorite form, as the amount of copper in the glazes increased (Fig. 1a). In addition, Tenorite crystallized as dendrites is observed in the samples cross section by using polarized light optical microscopy (inset in Fig. 1a). It is intuited that these crystallizations took place from the top of the glaze surface. A baseline rising between 20 and 35° 2θ in X-ray patterns corresponds to the presence of glassy phase as usual in glazes.

In regular low temperature luster obtained in reducing atmosphere the origin of the bright metallic effect are not completely understood. Some authors attribute the luster effect to the presence of Cu(0)[18] or Cu(I).[19] For the present study, the metallic

effect has been achieved by fast firing at 1200 °C in air. Under these conditions the appearance of metallic copper does not seem possible.

Fig. 1b shows the DTA/TG curves of S15. The peaks corresponding to the transformation of kaolin to metakaolin appeared at ≈500 °C (endothermic process accompanied by weight loss) and the transformation of the metakaolin to the spinel (exothermic process) occurred at 850 °C[20] (processes A and B in Fig. 1b). A weight gain corresponding to the oxidation of 98 wt.% of the initial metallic copper up to 900 °C (process C) was also observed, and a partial reduction of it near 975 °C (process D) corresponding to the 1.8 wt.% of the total copper calculated form Tg curve. Cu(I) is presented due to the presence of Na^+ into the glaze composition that favors the cationic exchange with the glassy matrix. The specie Cu(I) in an alkaline glaze could suffer dimutation that promotes the appearance of Cu(0). It is also reported that Cu(I) is able to be reduced to Cu(0) in glasses at temperatures near to 1070 °C.[21] In our case, the mass loss corresponding to this copper reduction has been estimated and it corresponds to about 0.2 wt.% of the total initial copper (process E), indicating that the metallic copper formed is very limited.

At higher temperatures the theoretical melting point of metallic copper at 1084 °C is also observed (process F). Therefore, after the reduction of Cu(II) the melting of the Cu(0) takes place. This melted copper oxidizes almost instantaneously. Taking into account these experimental results the presence of metallic copper nanoparticles is not expected in our glazes, that are fired at 1200 °C, in disagreement with those glazes sintered at lower temperatures.[22]

The oxidation state of copper affects the glass forming ability. The oxidation state, as Cu^+/Cu^{2+} ratio, depends on the glass composition, melting conditions (temperature, time, atmosphere and annealing history) and the concentration of copper.[23]

In agreement with low temperature lusters, the metallic effect takes place exclusively at the glaze surface as was previously described.[24] After slightly polishing the metallic glaze surface, it becomes black and lacks the luster effect. The coating thickness that shows metallic effect is about 70 nm in average, as determined by ellipsometry.

Previous reports[15,25] cannot exclude the presence of the different copper species Cu(0), Cu(I) and Cu(II) in lower temperature lusters. At higher sintering temperatures the role of the copper oxidation state in glass is still more complex.

A XANES study (Fig. 2) is afforded to determine the oxidation state of the copper on the coatings. The variation of the copper oxidation state with the depth in the glaze layer was studied by the variation of the beam incident angle over the surface. As references, metallic copper and stabilized Cu_2O and CuO (all of them from Aldrich) were measured and the results are shown in Fig. 2a in derivative form in order to better distinguish the energies at which the absorptions appear.

The absorption of metallic Cu k-edge XANES corresponds to 8979 eV and is assigned to the main 1s → 4p transition. Cu(II) is in a d^9 configuration and thus, Cu^{2+} presents a weak pre-edge corresponding to the quadruple allowed 1s → 3d transition.[26] Cu(0) and Cu(I) with a d^0 configuration have no hole in 3d orbital so this transition is not possible. Fig. 2b shows a com-

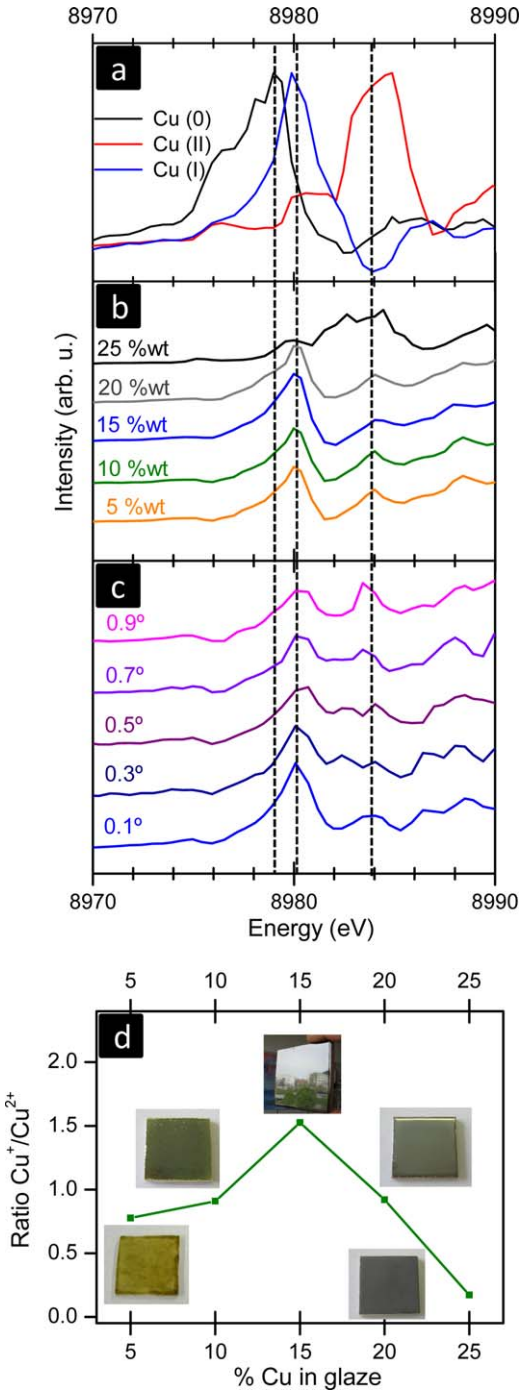

Fig. 2. XANES measurements of glazes: (a) metallic copper, Cu_2O and CuO as references. (b) Differences in the copper oxidation state in the samples: as the amount of copper in the glaze increases, the amount of Cu(II) also increases with respect to Cu(I). (c) XANES study of the glaze layer corresponding to S20 depending on the incident angle beam; in the surface, the specie Cu(I) is predominated over Cu(II) and as the beam penetrates more deeper in the sample the amount of Cu(II) increases. (d) The Cu^+/Cu^{2+} ratio obtained from XANES measurements of the sample surfaces reaches its maximum value for S15. The different aesthetical aspects of the glazes coatings depending on the weight percent of copper are also shown: yellowish sample corresponding to S5, green glaze (S10), bright metallic effect of S15, matt metallic effect of S20 and rough and matt surface of S25.

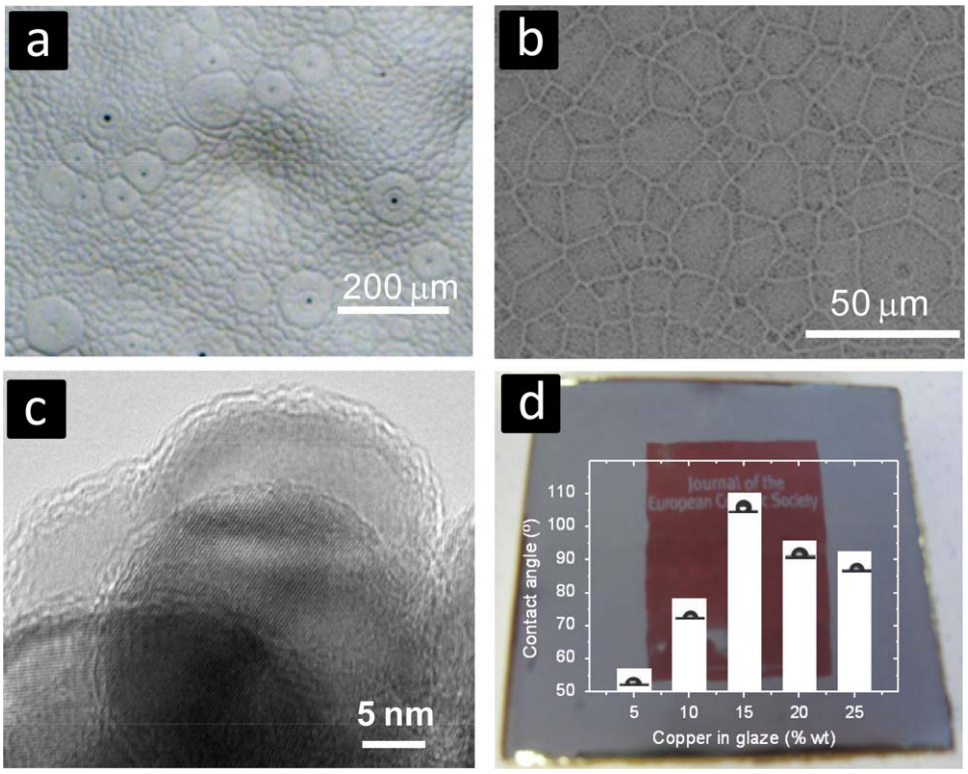

Fig. 3. (a) Polarized light optical microscopy of the surface with bright metallic shine (S15) where the microroughness is intuited. (b) "Cellular microstructure" of the surface of the S15 observed by FESEM. (c) Nanoparticles in the cellular microstructure of the surface of S15 by TEM corresponding to Tenorite nanoparticles. (e) Water contact angles of the glazes surfaces with different weight percents of copper added. As background, the reflection of the logo Journal of the Ceramic Society on a bright metallic glaze.

parative study of the XANES derivate of the glazes. Cu(I) and Cu(II) are present in the glaze coatings, but evidence of Cu(0) is very scarce. The highest amount of Cu(I) corresponds to the sample with metallic effect S15, whereas the S25 sample presents similar spectra to the reference CuO one.

Fig. 2c shows a study of the XANES derivate of the bright metallic effect sample (S15) measured in grazing incidence configuration[27] from 0.1° to 0.9°. By ellipsometry, a layer of 70 nm thickness has been found, so differences as the beam penetrates in the bulk of the glaze should appear. It can be observed that Cu(I) and Cu(II) are presented in all spectra, but Cu(0) was not observed. The surface of the bright metallic samples S15 presents a higher Cu(I)/Cu(II) ratio than in the bulk of the glaze. These data disagree with the ones described in the literature, where the metallic aspect was assigned to the presence of metallic Cu, but is consistent with the high temperature and oxidizing atmosphere used in our firing process. The lack of Cu(0) indicates that metallic nanoparticles do not remain after the sintering process.

The microstructure of the coating was observed by polarized light optical microscopy, see Fig. 3a. Yellowish and greenish samples do not show any surface microstructure as expected from their similarity with standard glazes. Sample with metallic shine effect (S15) presents a surprisingly characteristic microstructure that resembles cells (Fig. 3b), hereafter referred as cellular microstructure. This microstructure is similar to the one reported in different hydrophobic leaves, such as *Colocasia sculenta* or *Tropaeolum majus*.[28,29] The occurrence of this characteristic structure is exclusive for ceramic nanocoatings with bright metallic effect. Roughed surface sample S25 is absent of cellular microstructure (not shown), only irregular crystallizations of CuO are appreciated. The S20 coating shows an evolved cellular microstructure with crystallizations inside the cells that correspond to Tenorite phase, in agreement with XRD pattern evolution. When the glazes are slightly polished neither luster nor cellular microstructure are observed.

The cellular microstructure shows spherical nanoparticles forming a nanostructure in the samples, in a way similar to that of hydrophobic leaves. The main difference between S15 and S20 samples is the nanoparticle size. The samples with metallic shine effect present spherical particles of ≈30 nm in diameter (Fig. 3c). The fast firing sintering kinetically limits the nanoparticles growth. The driving force to form the nanoparticles at the surface is the crystallization from a saturated liquid phase in which the Cu(I) state predominated.

The nanoroughness of the surface coating produces changes in the water contact angle (Fig. 3d). The samples with the lowest amount of copper and flat glassy surface show hydrophilic behavior with contact angles of about 50°. S15, having bright metallic effect, presents the highest contact angle, about 115°, being then a hydrophobic ceramic nanocoating. For S20 and S25 glazes, the obtained values for water contact angles are over 90°. The nano and microstructure of hydrophobic leaves has been mimicked at the surface of the glazes with the crystallization

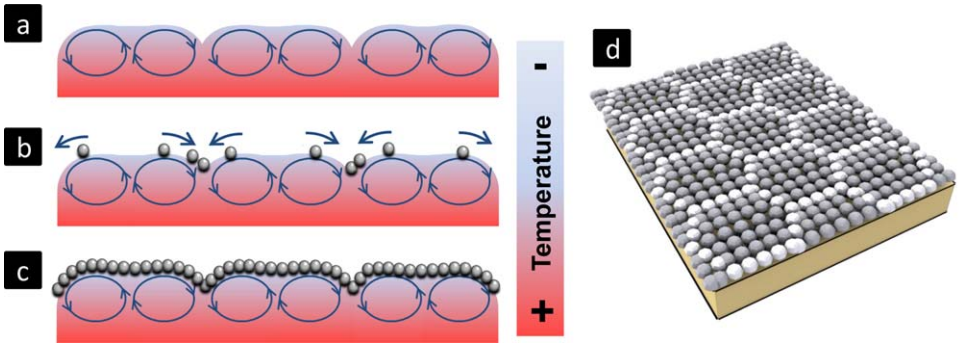

Fig. 4. Model representation of the formation mechanism for the cellular microstructure and the nanostructure for the bright metallic coating. (a) Rayleigh–Bénard currents in the top layer (lateral size of the sample). (b) Beginning of the Tenorite nanoparticles crystallization and their trend to be ordered by Rayleigh–Bénard currents (lateral size of the sample). (c) Nanoparticles ordering at the surface of the glaze after the crystallization process finished (lateral size of the sample). (d) Representation of the nanocoating where the Tenorite nanoparticles formed the cellular microstructure and the nanostructure.

of copper nanoparticles. It was described that a higher fraction of empty spaces below the water drop produces an increase of the contact angle between the drop and the surface, making the surface more hydrophobic.[30] This fact confirms that the S15 presents a higher hydrophobic value than samples with larger amount of copper.

The cellular microstructure is similar to the one found when Rayleigh–Benard[31,32] convection currents take place in the shallow copper rich layer. This is due to the differences of viscous forces and buoyancy. During the cooling step, the temperature is still higher in the bulk of the glaze than at the surface. This fact introduces a perturbation in the system that favor a convection gradient which is organized in periodic contrarotative rolls (Fig. 4a). These rolls, also known as Rayleigh–Benard cells, appear when there is a coupling between the dynamic field and the thermal field. Decreasing the temperature, nanoparticles of Tenorite begin to crystallize (Fig. 4b). When the Tenorite nanoparticles at the surface are formed the surface viscosity increases and the nanoparticles are impoverished of Cu. Therefore, Cu at the surface is limited and the nanoparticles growth is inhibited. Due to the movements organized in periodic contrarotative rolls the crystallized nanoparticles are ordered at the surface, forming the micrometric cells and the nanostructure aspect (Fig. 4c and d). The bottom-up process proposed allows the formation of a nano microstructure coating at the surface of copper-saturated glass matrix. This nanocoating combined metallic shine aspect with hydrophobic effect that correlated with a high Cu^{+}/Cu^{2+} ratio.

4. Conclusions

To summarize, ceramic nanocoatings having metallic effect and hydrophobic characteristics are performed in copper based glazes. A high temperature sintering process in oxidizing atmosphere is used. The multifunctional properties are ascribed to a bottom-up formation of micro and nanostructure at the surface of the glazes in which the Cu^{+}/Cu^{2+} ratio plays a main role in the control of nanoparticle size. The mechanism responsible for the micro-nanostructure is attributed to the kinetic conditions of Tenorite nanoparticles crystallization, due to the Rayleigh–Benard convections cells.

Acknowledgements

The authors are grateful to I. Lorite and P. Leret for their collaboration and discussion, and to M. Parrondo for his help in the figure of models. They are also grateful to F. Jimenez-Villacorta and J. A. Gallastegui for their very valuable help about the measurements in ESRF. Finally the authors would like to thank to the projects MAT2010-21088-C03-01 and CENIT DOMINO for the financial support.

Appendix A. Supplementary data

Supplementary data associated with this article can be found, in the online version, at doi:10.1016/j.jeurceramsoc.2011.08.013.

References

1. Pérez-Arantegui J, Larrea A, Molera J, Pradell T, Vendrell-Saz M. *Some aspects of the characterization of decorations on ceramic glazes. Appl Phys A* 2004;**79**:235–9.
2. Pradell T, Molera J, Bayés C, Roura P. *Luster decoration for ceramics: mechanisms of metallic luster formation. Appl Phys A* 2006;**83**: 203–8.
3. Pradell TJ, Molera J, Roque J, Vendrell-Saz M, Smith AD, Crespo D. *Ionic-exchange mechanism in the formation of medieval luster decorations. J Am Ceram Soc* 2005;**88**:1281–9.
4. Pérez-Arantegui J, Molera J, Larrea A, Pradell T, Vendrell-Saz M, Borgia I, et al. *Luster pottery from the thirteenth century to the sixteenth century: a nanostructured thin metallic film. J Am Ceram Soc* 2001;**84**:442–6.
5. Reillon V, Berthier S, Andraud C. *New perspectives for the understanding of the optical properties of middle-age nano-cerments: the lustres. Physica B* 2007;**394**:242–7.
6. Smith AD, Pradell T, Roqué J, Molera J, Vendrell-Saz MA, Dent AJ, et al. *Color variations in 13th century Hispanic lustre – an EXAFS study. J Non-Cryst Solids* 2006;**352**:5353–61.
7. Lim HS, Baek JH, Park K, Shin HS, Kim J, Cho JH. *Multifunctional hybrid fabrics with thermally stable superhydrophobicity. Adv Mater* 2010;**22**:2138–41.
8. Gao X, Jiang L. *Water-repellent legs of water striders. Nature* 2004; **432**:36.

9. Liu X, Jiang Z, Li J, Zhang Z, Ren L. *Super-hydrophobic property of nano-sized cupric oxide films*. *Surf Coat Technol* 2010;**204**:3200–4.
10. Crick CR, Parkin IP. *Preparation and characterisation of super-hydrophobic surfaces*. *Chem Eur J* 2010;**16**:3568–88.
11. Jaquotot P, Campillo A, Reinosa JJ, Romero JJ, Bengochea MA, Esteban-Cubillo A, et al. *Development of nanostructured multifunctional glazes*. *Bol Soc Esp Ceram V* 2009;**48**:95–8.
12. Santaren J, Limpo J, Aguilar E, Alvarez A, Moya JS, Pecharromán C, Patent ES2229940, 2006.
13. Pecharromán C, Esteban-Cubillo A, Montero I, Moya JS. *Monodisperse and corrosion-resistant metallic nanoparticles embedded into sepiolite particles for optical and magnetic applications*. *J Am Ceram Soc* 2006;**89**(10):3043–9.
14. Siligardi C, Montecchi M, Montorsi M, Pasquali L. *Lead free Cu-containing frit for modern metallic glaze*. *J Am Ceram Soc* 2009;**92**:2784–90.
15. Cable M, Xiang ZD. *Optical spectra of copper ions in alkali-lime-silica glasses*. *Phys Chem Glasses* 1992;**33**:154–60.
16. Macalik B, Krajczyk L, Morawska-Kowal T. *Colloidal copper in soda-lime silicate glasses characterized by optical and structural methods*. *Phys Status Solidi* 2007;**4**:761–4.
17. Ravikumar RVSSN, Komatsu R, Ikeda K, Chandrasekhar AV, Ramamoorthy L, Reddy BJ, et al. *Spectroscopic studies of copper-doped $ARbB_4O_7$ (A = Na, K) glasses*. *Phys Rev B: Condens Matter* 2003;**334**:398–402.
18. Polvorinos del Río A, Castaing J, Aucouturier M. *Metallic nano-particles in lustre glazed ceramics from the 15th century in Seville studied by PIXE and RBS*. *Nucl Instrum Methods Phys Res Sect B* 2006;**249**:596–600.
19. Padovani S, Sada C, Mazzoldi P, Brunetti B, Borgia I, Sgamellotti A, et al. *Copper in glazes of Renaissance luster pottery: nanoparticles, ions and local environment*. *J Appl Phys* 2003;**93**:10058–63.
20. Reinosa JJ, Rubio-Marcos F, Solera E, Bengochea MA, Fernández JF. *Sintering behaviour of nanostructured glass–ceramic glazes*. *Ceram Int* 2010;**36**:1845–50.
21. Wendlandt WWM. Thermal analysis. 3rd edition New York: Wiley & Sons; 1986.
22. Roqué J, Pradell T, Molera J, Vendrell-Saz M. *Evidence of nucleation and growth of metal Cu and Ag nanoparticles in lustre: AFM surface characterization*. *J Non-Cryst Solids* 2005;**351**:568–75.
23. Metwalli E. *Copper redox behavior, structure and properties of copper lead borate glasses*. *J Non-Cryst Solids* 2003;**317**:221–30.
24. Malins JP, Tonge KH. *Reduction processes in the formation of lustre glazed ceramics*. *Thermochim Acta* 1999;**340**:395–405.
25. Gonella F, Quaranta A, Padovani S, Sada C, DĭAcapito F, Maurizio C, et al. *Copper diffusion in ion-exchanged soda-lime glass*. *Appl Phys A* 2005;**81**:1065–71.
26. Vaseem MA, Umar A, Hahn YB, Kim DH, Lee KS, Jang JS, et al. *Flower-shaped CuO nanostructures: structural, photocatalytic and XANES studies*. *Catal Commun* 2008;**10**:11–7.
27. D'Acapito F, Davoli I, Ghigna P, Mobilio S. *The reflEXAFS station at the GILDA beamline (BM08) of ESRF*. *J Synchr Rad* 2003;**10**:260.
28. Koch K, Bhushan B, Barthlott W. *Multifunctional surface structures of plants: an inspiration for biomimetics*. *Prog Mater Sci* 2009;**54**:137–78.
29. Neunhuis C, Barthlott W. *Characterization and distribution of water repellent self cleaning plant surfaces*. *Ann Bot* 1997;**79**:667–77.
30. Bushan V, Yong Chae Jung, Koch K. *Micro-, nano- and hierarchical structures for superhydrophobicity, self-cleaning and low adhesion*. *Philos Trans R Soc A* 2009;**367**:1631–72.
31. Dinh TN, Yang YZ, Tu JP, Nourgaliev RR, Theofanous TG. Rayleigh–Bénard natural convection heat transfer: pattern formation, complexity and predictability. In: *Proceedings of ICAPP'04*. 2004. Paper 4241.
32. Cartwright JHE, Piro O, Villacampa AI. *Pattern formation in solutal convection: vermiculated rolls and isolated cells*. *Physica A* 2002;**314**:291–8.